

## A Julia set model of field-directed morphogenesis: developmental biology and artificial life

Michael Levin

### Abstract

*One paradigm used in understanding the control of morphogenetic events is the concept of positional information, where sub-organismic components (such as cells) act in response to positional cues. It is important to determine what kinds of spatiotemporal patterns may be obtained by such a method, and what the characteristics of such a morphogenetic process might be. This paper presents a computer model of morphogenesis based on gene activity driven by interpreting a positional information field. In this model, the interactions of mutually regulating developmental genes are viewed as a map from  $R^2$  to  $R^2$ , and are modeled by the complex number algebra. Functions in complex variables are used to simulate genetic interactions resulting in position-dependent differentiation. This is shown to be equivalent to computing modified Julia sets, and is seen to be sufficient to produce a very rich set of morphologies which are similar in appearance and several important characteristics to those of real organisms. The properties of this model can be used to study the potential role of fields and positional information as guiding factors in morphogenesis, as the model facilitates the study of static images, time-series (movies) and experimental alterations of the developmental process. It is thus shown that gene interactions can be modeled as a multi-dimensional algebra, and that only two interacting genes are sufficient for (i) complex pattern formation, (ii) chaotic differentiation behavior, and (iii) production of sharp edges from a continuous positional information field. This model is meant to elucidate the properties of the process of positional information-guided biomorphogenesis, not to serve as a simulation of any particular organism's development. Good quantitative data are not currently available on the interplay of gene products in morphogenesis. Thus, no attempt is made to link the images produced with actual pictures of any particular real organism. A brief introduction to top-down models and positional information is followed by the formal definition of the model. Then, the implications of the resulting morphologies to biological development are discussed, in terms of static shapes, parametrization studies, time series (movies made from individual frames), and behavior of the model in light of experimental perturbations. All figures (in grayscale),*

*formulas and parameter values needed to re-create the figures and movies are included.*

### Introduction

#### *The biology of artificial life*

Computer models can serve as biological theories (as in Garfinkel, 1984; Partridge and Lopez, 1984). The rapidly growing field of artificial life uses computer models to emphasize the common processes and characteristics of living things, rather than their physico-chemical implementation. The accent is on the role of bioinformation, cybernetic control processes, complexity and systems theory, rather than the study of specific instances of physicochemical processes (Apter, 1966; Goel and Thompson, 1986; Langton, 1990, 1991).

Computer simulations provide the experimental biologist with a much needed means for doing experiments on theories. We usually think of experiments as something performed on cells, to determine whether the cells' responses will match predictions made by a theory. However, when dealing with complex phenomena and with correspondingly complex theories, what a given hypothesis predicts can be less than obvious. It can be even more difficult to perceive which components in the hypothesis give rise to a particular prediction, much less to know what alternative classes of hypothesis would have predicted the same results. Lastly, anyone with sufficient insight to predict the consequences of a given theory may need objective methods for providing it to others. Computer simulations can help solve all these problems. (Harris, 1990)

This approach is at the intersection of biology, mathematics, physics and computer science, and has mainly involved computer models of behavior or evolution. Some attempts to model various developmental phenomena (cell proliferation, cleavage, cell migration, specific pattern formation, etc.) by creating computer simulations of the behavior of the underlying components have been made (Ransom, 1981; Meinhardt, 1982, are good summaries of such efforts). Interesting special cases are found in Düchting and Vogelsaenger (1984, 1985) and Thom (1983). Good examples of the common 'bottom-up' model (where the desired phenomenon emerges from a simulation of empirically derived behaviors of lower-level

components) can be found in Goel and Roger (1978) and Rogers and Goel (1978).

In the 'top-down' model (sometimes termed 'informal'—Conrad, 1981), the researcher creates a computer simulation which behaves like the system modeled (in some interesting way), without too much regard for the empirical validity of specific *lower-level* components: the model's empirical fitness is tested at a higher level. This approach can be used to study characteristics of processes or general schemes. For example, one may create a well-fitting model of some animal's social behavior based on general principles of co-operation, game theory and information theory, without any regard as to whether the components of the equations have any physical counterparts in the animal's brain (e.g. Krebs *et al.*, 1978; Axelrod and Hamilton, 1981). These kinds of models usually precede bottom-up models, and are much more common in ethology, evolutionary theory and the cognitive sciences than in developmental biology. Excellent examples of top-down models are given in Raup and Michelson (1965), Rozenberg and Salomaa (1986) and Slack (1991). L-systems (Lindenmeyer, 1989; Prusinkiewicz and Lindenmeyer, 1990) are among the best examples of top-down models because they possess the appropriate higher-order behavior even though there is no known physical mechanism in plants which explicitly implements the symbol manipulation rules used in an L-system.

Whereas the bottom-up model tries to be as realistic and focused as possible, providing empirically accurate data of some narrow and specific aspect of development (e.g. Meinhardt, 1984; Ransom, 1984), the top-down model attempts to derive the overall pattern of control, information flow and higher-order characteristics at the cost of losing some lower-level realism. Bottom-up models are able to provide more concrete information about some narrowly defined process; the benefit of the top-down model is that it allows insight into the higher-order properties of processes, and can be used when sufficient data and/or theory for a bottom-up model is not available. These models are useful in the study of developmental morphogenesis because embryonic development is very likely to involve general mechanisms of increasing complexity; at the same time, much low-level data (such as quantitative mechanisms of gene interactions) are currently unavailable. This paper presents a positional field-driven model of development which is intermediate between the bottom-up and top-down types.

#### *Positional information and field concepts in biology*

The basic problem of pattern formation can be viewed from one (or a combination) of two general perspectives. The developing organism's resulting morphology can be seen as a product of subunits following a sort of master plan—a blueprint (at some level of detail) of the whole organism. Or, it may be an emergent phenomenon, where the overall pattern emerges as the result of purely local interactions between subunits governed by rules which say nothing about the overall pattern

(best exemplified by cellular automata systems, as in Gutowitz, 1991).

An intermediate paradigm involves positional information (Wolpert, 1969, 1971, 1989). That is, each unit (usually thought of as a cell, but this could apply equally well to tissues, cell sheets or subcellular components) is able to determine its position within the organism, and act (differentiate, migrate, proliferate, etc.) based upon that positional information. The positional information is usually thought of as coordinates in a field, which then can be a mechanism for long-range control and information transfer (see Cooke, 1975, for a review of field theories in biology). The paradigm is thus a combination of the two approaches in that it includes both purely local decision-making (with an emphasis on the distinction between the field itself, and various components' responses to it), as well as a global entity (the positional information field itself). In this view, the overall morphology emerges from units following rules which specify actions based on the unit's position; the process of morphogenesis can be 'characterized as a series of solutions of the morphogenetic field whose superposition gives way to complex stable patterns' (Goodwin, 1988). The role of positional information in early development is reviewed in Bard (1990) and Slack (1991); there is also evidence that adult animals maintain positional information cues (Harrison, 1918; Raff and Kauffman, 1983).

The field is a very attractive theoretical construct for modeling global influences and thus explaining static stability as well as temporal change of a complex morphology, and the ability of numerous processes to combine into a coherent whole and to tend toward that configuration when experimentally perturbed (Goodwin, 1985):

In real organisms, there must at critical times or even continuously be an overlay of global instructions that keeps the ramifying network of inductive interactions in the correct relationship by specifying reference to whole-organism properties. (Thomson, 1988)

Fields have recently become truly useful in the study of development through mathematical models (see, for example, French *et al.*, 1966; Goodwin and Cohen, 1969; Goodwin and Trainor, 1980; Ransom, 1981; Trainor, 1982; Goodwin and LaCroix, 1984; Goodwin *et al.*, 1987; Nagorcka, 1989; Brandts and Trainor, 1990a,b) and empirical confirmation of their existence and crucial role in development (Burr, 1941; Lund, 1947; Cooke, 1972a–c, 1973a–c; Jaffe, 1979; Kropf and Caldwell 1983; Nucitelli, 1986; Gow, 1987). Field theories are useful in explaining the phenomena of cleavage (e.g. Goodwin and Trainor, 1980), regeneration (e.g. Tevlin and Trainor, 1985; Mittenthal and Nuelle, 1988), supernumerary limb production (e.g. Bryant and Iten, 1976; Mittenthal and Trevarrow, 1984; Gardiner and Bryant, 1989), and cancer and malignancy (Matioli, 1987).

Two interesting top-down field-based models are given by Evans (1986) and Thompson (1961). Evans' model involves generation of morphologies very similar to that of the human fetus, based on electromagnetic field characteristics of the nervous system. Thompson (1961) and Palmer (1957) show that it is possible to convert between the morphologies of various existing animals by applying simple mathematical deformations to their two-dimensional field representations. Field theories must specify several characteristics of the process: the physical nature of the field; what exactly perceives this information; what the time characteristics of field perception are; and how the field is in turn modified by the units that read it.

A field can consist of a chemical morphogen gradient or system of gradients (e.g. Russel, 1985; French, 1988; Green *et al.*, 1992), an electromagnetic field (patterns of ionic currents and potential differences, e.g. Nucitelli, 1984, 1986), an osmotic field (O'Shea, 1988), a field of differential adhesiveness (haptotactic fields, as in Murray and Oster, 1984; Zackson and Steinberg, 1988; Lord and Sanders, 1992) or a visco-elastic tension field (e.g. Lakirev and Belousov, 1986; Hart *et al.*, 1989; Brière and Goodwin, 1990). The salient point is that there is some physical factor which forms a field throughout the embryo (though it is not necessarily the case that every part of the embryo utilizes the information in it), such that units (cells, for example) can interact with it and thus obtain information about their position within the embryo. The model described in this paper is not committed to any specific physical nature of the field; it applies to all Cartesian fields.

The basic unit of field-reading need not necessarily be individual cells. It may be a subcellular component (e.g. Frankel, 1974), or a cell group or sheet (as in Hart and Trainor, 1989). The temporal characteristics of field reading have also been studied, e.g. Savel'ev (1988) shows that neuroepithelial cells in the amphibian brain read their positional information (in this case, maintained as a mechanical strain field) at discrete times, exhibiting time-limited field perception events. This model likewise assumes the field interpretation to occur in discrete steps. The dynamics of interactions between sources of positional information fields and the fields themselves are a very important topic. As a simplifying assumption, however, in this paper the focus will be on an existent static field and the interactions of receivers with the information it carries.

Many attempts to model specific developmental processes exist (see Ransom, 1981; Meinhardt, 1982, for reviews). Some are based on continuous functions and differential equations (such as Yates and Pate, 1989), while others are based on finite-state automata and discrete finite-mathematical methods (e.g. Herman and Rozenberg, 1975; MacDonald, 1983). Although the field concept has been useful in various specific applications, it is an open question as to whether positional information in general can account for the morphological complexity of real organisms. In order to assess the potential role and implications of field theories in development, it is first

necessary to show that this type of mechanism is capable of generating the kind of order found in biological morphogenesis. It is also interesting to examine some of the features of the morphogenetic process which is controlled in this way. To these ends, a computer model was developed. This model turned out to be remarkably similar to algorithms used to generate fractal images, which have been extensively used to model complete biological shapes (e.g. Prusinkiewicz and Lindenmeyer, 1990).

The original model described in this paper attempts a wider view of the control processes of development, by modeling cell decisions controlled by field-specified positional information. The model has a strong bottom-up component in that it is based on a process which is known to be crucial in biomorphogenesis—determination of cell fates via gene interactions. It is top-down in that it is not a simulation of any specific actual organism, but of a *type of process*—positional information interpretation based on genetic interactions. It is not being claimed that the specific formulas (used below) describe any existent organism; rather, it is a computer implementation of a possible morphogenetic control process. Thus, the strength of the model is *not* based on the fact that the images produced may look like biological forms, but lies in the fact that the model can be used to study the higher-order properties of field-directed gene interactions in morphogenesis. It makes several concrete predictions, and explains several key phenomena. When quantitative information on morphogenetic gene interactions becomes available, this can be used within the context of the model described herein to make concrete predictions about specific organisms.

### The Julia set model

#### *Interpretation*

Morphogenesis is seen to be a three-stage process: (i) a positional information field is specified (by factors in the external environment, by the mother's organism, or by components within the embryo itself); (ii) cells go through a complex set of genetic interactions and phenotypic effects, and then achieve some final genetic state based on their positions within this field; and (iii) this genetic state determines the behavior of the cell (migration, proliferation, apoptosis, adhesion, etc.). The mechanical interactions of the cells finally determine the overall morphology of the organism.

The current model consists of a computer algorithm which simulates cell behavior within a field. Each cell finds itself within some unique position in a two-dimensional field; a mathematical function (shown to be isomorphic to a modified Julia set, after Pickover, 1990) then describes the behavior of the cell at that position. Of course it is not being suggested that there is a mechanism within the cell that computes this function in the sense of formal computation; rather, the function is descriptive of the cell's behavior (much as Newton's laws describe the motion of the moon, without any need for the moon

formally to compute the functions). This model is similar to Thompson's (1961) model since applying the deformations to the axes is equivalent to applying a deformation to the coordinate points making up the image. Thus, Thompson's model also represents a positional-field interpretation model, but is different from the model presented in this paper because his model applies a deformation to an existing form, while the model described here generates the morphology *de novo*.

Specifically, the simulation works as follows. In achieving some fate, each cell goes through a complex cycle of reactions between various key gene products (similar to that in Kauffman, 1969). Below, 'gene interactions' refers to regulation of expression of gene products by other gene products in a mutually regulating network. Thus a cell at a certain time can be viewed as being controlled by a collection of concentrations of gene products  $\langle P_1, P_2, \dots \rangle$ , which interact in time to up- and down-regulate each other's expression. These interactions can be viewed as the instantiation of a function  $\Phi()$  which converts a given cell state  $\langle P_1, P_2, \dots \rangle$  into a different cell state  $\langle P'_1, P'_2, \dots \rangle$  with passage of time (which, as a simplification, is taken to be discrete). The cycle of interactions between the genes which finally stabilizes with some differentiation path is modeled by applying the function  $F$  recurrently to some initial (totipotent) cell state, until a stable point is reached. The stable point can be an instance of one of two possibilities. After  $N$  cycles, either some of the gene products have increased beyond a certain threshold and activated a specific program (the cell has differentiated into a specific fate), or this has not happened, meaning that the cell is like a stem cell—it stays perpetually undifferentiated.

In this model, only two gene products are considered,  $X$  and  $Y$ . Though in reality a larger set of genes is clearly responsible for the morphogenesis of features in organisms, it is one of the important results of this study that two genes are sufficient to produce a very rich set of morphologies with properties similar to those of real morphogenetic processes. Each cell is at a certain position  $x, y$  within the field (two-dimensional, as a simplification). This position is interpreted (perhaps by a mechanism similar to that of Hox genes, as in Tabin, 1991) to arrive at a specific initial concentration of two gene products,  $\langle X, Y \rangle$ . Then, a function is applied (simulating gene regulation) which alters  $X$  and  $Y$  in an interdependent manner (e.g. it might map  $X_i$  to  $X_{i-1} - c \cdot Y_{i-1}$ , modeling a linear inhibition of expression of  $X$  by the product of  $Y$ ). The function is taken to be a map in complex numbers (thus an  $N$ -dimensional algebra can be defined for modeling the interactions of  $N$  genes), so that  $\langle X, Y \rangle$  is represented as  $X + Y_i$ , and is applied for a number of iterations. At the end, either the magnitude of  $X$  or the magnitude of  $Y$  has reached a certain threshold value, or neither has. Whether the limit has been reached, and if so, how quickly, determines the 'type' of the cell. This algorithm is extremely similar to one used in generating various fractal images, and is isomorphic to Julia set computation.

### Fractals in biology

Julia sets are generated by a fractal algorithm, and are closely related to Mandelbrot sets. While the mathematics behind these objects is fairly well researched, their higher-order (morphological) characteristics are relatively poorly understood. Some considerations of the mathematical properties of complex iterations are found in Beardon (1990, 1991). This is a new (the first articles began to appear around 1968) and very active topic in mathematics. Fractals' main features are widely differing behaviors for close initial points (chaos, due to their recursiveness which magnifies small differences), their production of images that are self-similar in regions, and the incredible richness of structures, which is produced by very short formulas (Peitgen and Saupe, 1988). Note that fractals' chaotic behavior provides a possible answer to the question (Lewis *et al.*, 1977) of how a smooth (continuous) field can give rise to discrete cell states (the problem of sharp thresholds): the potential for two very close complex field values to have widely different fates under iterative transformations is a hallmark of fractal (chaotic) algorithms. Thus, after a time of genetic interactions, two close cell states  $\langle X, Y \rangle$  and  $\langle X', Y' \rangle$  can diverge to become widely differing cell types, providing sharp differentiation boundaries within a continuous field.

Fractal algorithms are highly 'epigenetic', and the generativity is uni-directional. That is, given a fractal formula it is very easy to produce the complex morphology it codes for (as a complex biological organism is formed as a result of chemical reactions driven by the information content of DNA); however, given a complete morphology, it is exceedingly difficult to find a short formula that codes for it (as would be very difficult, given the morphology of an organism, to determine the content of the DNA which would produce that organism). The same sort of reason that may explain why there is no inheritance of acquired characteristics (that the epigenetic character of development makes it nearly impossible to translate directly some characteristic of an organism back into its DNA) makes it very difficult to find a fractal formula coding for some given morphology.

The fact that Julia sets map positions in a plane to discrete scalar values by iterating interdependent changes of several independent values makes them a natural candidate for a positional information model of pattern formation due to differential gene activation. Pietronero and Tosatti (1986) and Feder and Aharony (1990) present overviews of the importance of fractals in the study of physical processes. Fractal and chaotic algorithms form the basis for many physical processes important in development, such as diffusion-limited aggregation (Witten and Sander, 1981; Witten and Cates, 1986), viscous fingering (Sander, 1987) and percolation (Oxaal *et al.*, 1987). A great sourcebook for this information is the classic Mandelbrot (1982). These algorithms have been used in modeling and analyzing biophysical systems [e.g. ion channel activity (Liebovitch and Töth, 1990), neural activity (Ishibashi *et al.*,

1988) and dielectric response in biological tissues (Dissado, 1990)], various biological phenomena [e.g. periodontal disease (Landini, 1991), metabolism (Sernetz *et al.*, 1985; and for many more examples, West, 1991)], evolution (Green, 1991) and the development of different components of embryos, such as nerves, blood vessels and mosaic organs (see, for example, Meakin, 1986; Mainster, 1990; Iannaccone, 1990; Burlando *et al.*, 1991; Kiani and Hudetz, 1991; Smith *et al.*, 1991; Vaidya *et al.*, 1991).

Complex systems (of which biological organisms are the quintessential example) have several characteristics: 'they have many attributes with complex interdependencies and rules of interactions which are non-obvious, they are usually non-linear, and their dynamics appear stochastic, random, or fuzzy' (Goel and Thompson, 1988). These aspects are admirably captured by Julia set behavior.

The hypothesis that the differentiation pathway for a cell is determined by iterative chaotic processes has an interesting consequence, mirroring a similar result in the theory of dynamical systems. While for any given cell the final outcome (i.e. which differentiation fate is taken) is physically predetermined, in certain (though not all) cases it may be impossible to know what that outcome will be, even with good data about the initial gene product concentrations, since the gene interactions are iterative and thus magnify minute differences in initial conditions. Two widely divergent differentiation pathways may thus result from very close (and perhaps indistinguishable within some technique's precision) gene activity levels.

#### *The formal definition of the Julia set model algorithm*

The basic algorithm is as follows: for each position in the field (it is assumed that the field overlays a rectangular patch of cells, with every position occupied), the formula is applied, and the resulting cell behavior (e.g. a differentiation) is plotted at that position as a given color. The mapping of cell 'types' to colors is arbitrary. In pseudocode:

```
for each  $X$  from  $X_{\min}$  to  $X_{\max}$ 
  for each  $Y$  from  $Y_{\min}$  to  $Y_{\max}$ 
    plot a point at  $(X, Y)$  in a color  $T$  depending on  $\Phi(X, Y, \nu)$ 
```

Thus, the function  $\Phi()$  maps each position  $(X, Y)$  and a constant  $\nu$  to a type  $T$ .  $X$  and  $Y$  are varied within some range of values, and there is a finite and discrete number of types  $T$ . This corresponds to the biological case of a continuous population of primitive (undifferentiated), non-motile cells, within a two-dimensional positional information field, which differentiate as a function of their position in the field.

Thus, formally a given morphology is a quintuple  $M = \langle \lambda, \Phi, \nu, R, T \rangle$ , where:

- $\lambda$  is the field limitation—the domain of the field values seen by the subunits (upper and lower bounds on  $X$  and  $Y$  values

for the points examined). In terms of biological development, this expresses the boundaries on the field values that cells experience.

- $\Phi$  is the function—a mathematical function describing the input–output relation between the cell's position and its resulting type (describing the cell's mechanism for interaction with the field, some type of receptor, or membrane mechanism, which is determined by the cell's DNA). This function performs the iteration of the initial  $X, Y$  values through some complex formula.
- $\nu$ , the constant used in the function, represents some existing identical information all of the cells have when they begin morphogenesis.
- $R$  is the resolution, which determines how many points in the interval from  $X_{\min}$  to  $X_{\max}$  and  $Y_{\min}$  to  $Y_{\max}$  are sampled. In terms of biological systems, this parameter specifies how much of the morphology is a result of field–cell interactions, and how much is to be provided by purely local interactions which fill in the spaces between the field-specified points.
- $T$  is the set of possible cell behaviors (differentiation pathways).

#### *Computer implementation*

In a computer program, the field is implemented as the  $R^2$  space—a plane where each point corresponds to a complex number  $a + bi$ . Thus, for each point there is an  $X$  and  $Y$  value (corresponding to the concentrations of two different and orthogonally diffusing chemicals, in a morphogen field, for example, or the adhesiveness of two separate surfaces, in a tactile field). The function that is applied to the locations in the field is, in this model, a modified Julia set calculation [which differ from true Julia sets in that a point is plotted if and only if  $|\text{real}(z)| < \text{limit}$  or  $|\text{imaginary}(z)| < \text{limit}$ ]. That is, for each given point (complex number)  $Z$ , its value is recursively iterated through a formula such a  $z = z^2 + \nu$ , and the original point  $Z$  is plotted in a color which is related to how many iterations occurred before  $|z|$  exceeded some limit value. Some formal theory regarding these functions can be found in Beardon (1991).

Note that the images thus produced are those of pre-pattern—they are analogous to an *in situ* mRNA hybridization because they are showing final *genetic states* of cells, not what the organism actually looks like. The real morphology of an organism is derived from this pre-pattern by cell movements, mechanical deformations, apoptosis, etc., which are governed by the genetic states of the cells.

This limit value is a constraint on which points appear in the final image, and its biological interpretation is thus as a measure of the importance of the positional information. A high limit value would allow relatively many points to be placed, indicating that cells' fates are heavily influenced by the positional information. A low limit value would allow relatively few points

**Table I.** Formulas and parameter values

No.	Formula	X limits	Y limits	$\nu$ value	i-limit
1	$\text{conj}(z)^{4/3} +  z ^z + \nu$	-7.0 to 7.0	-7.0 to 7.0	(3.5,0)	100
2	$z^{9.5} + \sin(z) + \nu$	-1.5 to 1.5	-1.5 to 1.5	(2,-3)	60
3	$\sin(z) + e^z + \nu$	-2.398 to -2.433	1.73 to 1.765	(5,-3)	100
4	$e^{z \cdot \tan(z)} + z^{4.5} + z^{5.5} + \nu$	0.2 to 0.8	0.2 to 0.95	(0,0)	30
5	$z^{9.5} + \cos(e^z) + \nu$	-1.3 to 1.3	-1.3 to 1.3	(2,0)	100
6	$z^{8.5} + z^{0.5} + \nu$	-1.1 to 1.1	-1.1 to 1.1	(0,0)	20
7	$z^4 + \sin(z) + \nu$	-2.5 to 2.5	-2.5 to 2.5	(0,-26)	100
8	$\sin(z^{0.5}) + z^3 + \nu$	-3.2 to 3.0	-3.2 to 4.0	(0,0)	100
9	$z^{\text{conj}(z)} + z^2 + \nu$	-4.3 to 4.3	-5 to 5	(0,0)	25
10	$\sin(2 \cdot z) + z^2 + \nu$	-9 to 9	-6 to 6	(0,0)	100
11	$z^{2.6} + \sin(z) + (e^z)^{1/4} + \nu$	-9 to 8	-8 to 8	(0.2,1.7)	20
12	$z^{2.5} + \sin(z) + (e^z)^{0.7} + \nu$	-8 to 8	-8 to 8	(-0.2,2.7)	18
13	$z^2 + \sin(z) + \nu$	-12 to 12	-8 to 8	(-3.7,5.0)	100
14	$z^2 + \sin(z) + \nu$	-3.0 to 8.0	-0.5 to 5.5	(-9,-12.7)	100
15	$z^2 + \cos(z) + \nu$	-5.17 to -2.77	0.69 to 5.5	(3.2,8.7)	100
16	$\text{conj}(z)^{4/3} +  z ^z + \nu$	-1.2 to -0.2	0.1 to 1.4	(3.5,0)	20
17	$\sin(z) + e^z + \nu$	1.3 to 4.7	1.0 to 4.0	(5,-0.2)	100
18	$\sin(z)^3 + e^z + \nu$	-7.0 to 7.0	-5.0 to 5.0	(5,-0.8)	10
19	$z^{5.5} + \cos(z) + \nu$	-1.5 to 1.5	-1.8 to 1.8	(0,0)	100
20	$z^3 + \nu$	-1.6 to 1.6	-1.6 to 1.6	(-0.5,-2.0)	100
21	$z^3 + z^6 + \nu$	-1.1 to 1.1	-2.0 to 2.0	(0.5,0)	100
22	$z^3 + \nu$	-3.0 to 3.0	-3.0 to 3.0	(0.5,-1.0)	100
23	$z^{5.2} + \sin(5z) + (e^z)^{0.8} + \nu$	-3.5 to 3.1	-3 to 2.5	(0,0)	15
24	$z^2 + e^z + \nu$	3.15 to 3.7	2.05 to 3.0	(5.0,-0.2)	45
25	$z^{8.5} + z^{3.5} + \nu$	-0.03 to 0.0	-0.04 to 0.0	(0,0)	20
26	$\sin(z) + e^z + \nu$	-8.0 to 8.0	-8.0 to 8.0	(1,-2)	100
27	$z^{1/z} +  z ^z + \nu$	-5.0 to 5.0	-5.0 to 5.0	(0,0)	100
28	$z^{1/z} + z^3 + \nu$	-2.5 to 3.5	-2.5 to 3.4	(0,0)	100
29	$z^{1/z} + z^{2.5} + \nu$	-3.0 to 4.0	-3.9 to 3.9	(0,0)	100
30	$z^{1/z} + z \cdot \sin( z ) + z^{5.5} + \nu$	-1.15 to 1.5	-1.4 to 1.45	(0,0)	100
31	$z^{1/z} +  \epsilon^z ^z + \nu$	-6.0 to 6.0	-5.0 to 5.0	(0,0)	100
32	$z^{4.5} + \cos(z) + \nu$	-1.3 to -0.5	-0.5 to 0.22	(-1.5,-0.3)	100
33	$\sin(z) + e^z + \nu$	-35.0 to 15.0	-15.0 to 15.0	(-0.5,29)	30
34	$z^{8.5} + \nu$	-1.5 to 1.5	-1.5 to 1.5	(0,0)	20
35	$z^{8.5} + \text{conj}(z)^{3.3} + \nu$	-1.2 to 1.2	-1.2 to 1.2	(0,0)	20
36	$z^2 + z^6 + \nu$	-1.3 to 1.3	-1.0 to 1.0	(-0.3,0.8)	100
37	$z^2 + z^6 + \nu$	-1.3 to 1.3	-1.0 to 1.0	(-0.7,0.4)	100
38	$z^2 + \sin(z) + \nu$	-0.2 to 0.4	-0.2 to 0.2	(3.5,5)	100
39	$z^2 + \sin(z) + \nu$	-0.2 to 0.4	-0.2 to 0.2	(3.5,5.5)	100
40	$0.1z^{9.5} + 0.9 \cdot \sin(z) + \nu$	-1.55 to 0.55	-0.77 to 1.71	(2,-3)	60
41	$\text{conj}(z)^{4/3} +  z ^2 + \nu$	3.87 to 4.73	0.66 to 1.9	(3.5,0)	100
42	$\log \text{conj}(\sin(z))  + z^7 + \nu$	-0.8935 to 1.2277	-1.2172 to 1.108	(0,0)	100
43	$\log \text{conj}[\tanh(z)]  + z^7 + \nu$	-8.3 to 9.17	-9.8 to 9.7	(0,0)	100
44	$z^{3.5}$	-5.0 to 5.0	-5.0 to 5.0	(0,0)	100
45	$z^{3.5}$	-5.0 to 5.0	-5.0 to 5.0	(0,0)	100
46	$z^4 + \sin(z) + \nu$	-2.5 to 2.5	-2.5 to 2.5	(0,-26)	100
47	$z^4 + \sin(z) + \nu$	-2.5 to 2.5	-2.5 to 2.5	(0,-26)	100
48	$z^{3.5} + 1/\{\log \sin(z) \} + \nu$	-2.5 to 2.5	-2.6 to 2.6	(0,0)	100
49	$\exp(1/z^2) + \text{conj}(z)^{4.5} + \nu$	-1.65 to 1.56	-1.8 to 1.73	(0,0)	100
50	$z^{5.5} + 1/ \sin(z) $	-1.4 to 1.4	-1.5 to 1.5	(0,0)	100
51	$\cos( \epsilon^z ^z + z^{8.3})$	-1.4 to 1.18	-1.2 to 1.3	(0,0)	100
52	$\sin( \tan z ) + 1/(z^2) + z^{9.5}$	-2.7 to 2.7	-2.4 to 2.4	(0,0)	100
53	$\cos( \epsilon^z ) + (1/z) + z^{12.3}$	-1.8 to 2.0	-2.5 to 2.5	(0,0)	100
54	$z^{3.5} + 1/ \cos(z^3) $	-2.5 to 2.3	-2.2 to 2.2	(0,0)	100
55	$\sin( z )^2 + z^{3.3}$	-2.6 to 2.6	-2.6 to 2.6	(0,0)	100
56	$z^{1/\sin(z)} + e^z$	-2.62 to -2.55	3.572 to 3.694	(0,0)	100
57	$z^3 + \sin(z)^{32}$	-7.7 to 7.8	-1.1 to 1.1	(0,0)	100
58	$(e^z)^{3/2} + \text{conj}(z)^{8/8}$	-3.3 to 3.6	-3.66 to 3.6	(0,0)	100
59	$e^{z/\cos(z)} + \text{reverse}(z)^{9/8}$	-1.2 to 1.0	-1.2 to 1.2	(0,0)	100
60	$[z^{22} + \sin(z)]/z^{3.5}$	-0.472 to 0.205	0.7128 to 0.996	(0,0)	100
61	$z^{3.3} + \sin(z)^{w/z} + u$	-2.6 to 2.6	-2.6 to 2.6	(0.1,-0.2)	100

to be placed, indicating that only certain key cells get their fate specification from the positional field, the rest being determined by local near-neighbor interactions.

Note that the floating-point routines used in any computer's math library have a limit on their accuracy. This provides a natural limit to the differences in positional information that the cells will be able to detect, and corresponds to the limits in sensitivity of real cells to field values which differ by very small values.

It is important to realize that the formula in  $z$  is not identical with the function  $\Phi()$  mentioned above. The function  $\Phi()$  includes the formula, iteration and cutoff decision, and is used only once for each point; it maps a given  $(x,y)$  pair to a given type (color). The definition of  $\Phi()$  subsumes the iteration of the complex function, and the intermediate values of the real and imaginary components of  $z$  represent the concentrations of various gene products, as explained above.

The actual formulas used to produce the figures are shown in Table I. Note that on different computers certain parts of the pictures may look somewhat different than they do in the illustrations below. This is due to the accumulation of differences in machines' floating-point calculation errors (which are magnified due to the iterations of the formulas).

#### *Biologically relevant properties of morphologies produced by this model*

The figures show the variety of gene expression patterns that can be produced by only two gene products and a smooth linear Cartesian coordinate field. It is clear that this is sufficient to produce extremely rich patterns, which can be even further elaborated by cell movements and rearrangements to produce an embryo's final morphology. Of course it is not being suggested that all of the features observed in the figures are actually used in organisms' morphologies; rather these results show that the kinds of patterns found in biological systems can be plausibly produced by such a model.

#### *1. General notes on static shapes and how they resemble real organisms' morphologies*

Several general traits of these figures (see, for example, Figures 3–18) are similar to those of real organisms. Note how colors never merge—borders are well-defined; differentiation proceeds in layers, with distinct boundaries. There are clear borders between separate structures; there are many instances of objects possessing a definite inside and outside. There are almost no straight lines; curves predominate. As in real biological organisms, the morphology is an epigenetic phenomenon of the formula expressing the genetic interactions—it is very difficult to predict the large-scale morphological properties of the organism from the formula (genome).

Repeated magnification reveals ever more intricate detail, but every function described in this paper possesses a top-most view—a scale beyond which nothing interesting happens. This

indicates that for every organism, there are limits on which field values are valid (as perceived by the cells); the positional information field has definite edges. As in real organisms, there are recurrent spatial motifs—most of the images build on the same types of morphologies over and over again. Repeated segments are used in many images (see for example Figures 3, 24 and 57). Most figures show clear examples of structural hierarchies (a mathematical analysis of structural hierarchies in biological systems appears in Totaufurno *et al.*, 1980).

The symmetry properties of these functions are also reminiscent of life. Many images are truly symmetrical along one axis (as in Figures 5, 7 and 8); some are radially symmetrical (such as Figure 20). Some are regular, but not symmetrical along any axis (such as Figures 15 and 23). And others, such as Figure 27, seem to be bilaterally symmetrical, but close inspection reveals differences that break the symmetry (look closely at the distribution of the solid black sectors in Figure 27, and at the outgrowth to the right of Figure 59, reminiscent of the kinds of asymmetries found in crabs and lobsters); this resembles the morphology of many organisms that are bilaterally symmetrical, except for various features (such as the heart and liver in the human).

Many parts of the images are self-similar (see Figures 4 and 20), though are not exactly repeated units. There is usually some top-level shape, within which there are self-similar structures. Biological forms display many examples of self-similarity (for examples see West and Goldberger, 1987; Mandelbrot, 1982; Nelson and Goldberger, 1990; Guyon and Stanley, 1991; West, 1991). This self-similarity implies that the algorithm itself, with a given formula, dictates a specific shape, and this shape is basically the same in many regions of the field, at different resolutions. This means that (i) field values are relative, not absolute, and experiments with field-directed developmental systems can be done to test this; and (ii) parts of the field contain information for the whole organism.

This 'holographic' property of the model is interesting in light of the ability of many kinds of embryos (at certain stages) to regenerate from pieces, and recover the whole organism when pieces are removed. As with real embryos, not every region contains the crucial information, and only some regions can be 'magnified' into the proper morphology. Real embryos also possess this 'relativity' of positional information (e.g. in certain cases in early *Drosophila* axis formation, it is the relative concentrations of two morphogens which matter, not their absolute concentrations). During morphogenesis there is a 'matching of proportionate spatial structures to the size of the field in which the pattern is formed. It appears as if a size-sensing mechanism exists which controls and adapts the detailed structures in accordance with the variable field size, so that their relative extent remains invariant' (Papageorgiou and Venieratos, 1983). This is seen in the experiments on *Xenopus* (Cooke, 1973c, 1979, 1981), hydra (Bode and Bode, 1980) and a unicellular ciliate (Bakowska and Jerka-Dziadosz, 1980). How

might this property be supported by a morphogenetic field? In general, patterns generated by diffusion reactions are very sensitive to changes of scale. However, a variation on Turing's early model (Othmer and Pate, 1980) of spatial formation based on morphogen reaction-diffusion systems also exhibits scale invariance. A theoretical basis for morphogen gradient fields that exhibit scale invariance is given in Papageorgiou and Venieratos (1983).

In general, these images show that only two interacting genes are sufficient to produce rich morphologies from a smooth and continuous positional information field. This is an important result because it provides a convenient and biochemically plausible mechanism for how organic complexity arises from two simple orthogonal vectors.

Figure 34 shows a low-structure morphology. Note the simple circular layers of aggregated (mixed-color) tissue, and the simplicity of the formula by which it is produced. Not also that the image is radially symmetrical, except for a small horizontal line on the right. Figure 35 shows the same formula as Figure 34, with an additional component. Notice that this is a somewhat more complicated morphology, with modifications to the simple circular membrane of Figure 34, but still much simpler than any of the other figures.

Figures 36 and 37 show two morphologies which correspond to gene interactions that fail to produce coherent morphologies. Note the failure of layers to join in many places, and the confused disordered arrangement of internal detail (especially apparent in Figure 37). Another interesting example is seen in Figure 41 (this is just a magnification of the area overlaid by the dashed rectangle in Figure 1): note the complex behavior that occurs where two separate structures overlap. This should be studied further in light of the competing field influence found in *Xenopus* (Cooke, 1972a–c, 1973a,b).

## 2. Parametrization: how forms change in response to parameter changes

An important set of questions can be answered by this model through parametrization studies. The role of a given component (gene interaction rule) in producing the morphology can be studied by tracking the changes in the image as its value is slowly changed. Several things can be studied in this way: constants in the formula itself, the limit used in the cutoff point, the intercellular constant ( $\nu$ ), etc. The parametrization studies described below show that smoothly changing gene co-regulation functions from  $R^2$  to  $R^2$  are sufficient to produce the kinds of spatiotemporal processes that are observed in biological embryogenesis.

It is seen that for functions of the form  $z = z^n$  where  $n$  is small (between 1.0 and 4.0), changing  $\nu$  from  $0 + 0i$  serves to produce a very rich morphology from an otherwise monotonous one. This suggests that for these kinds of morphologies, field-independent information is an important determinant of form. However, for higher values of  $n$ , making

$\nu$  different from  $0 + 0i$  serves to disrupt severely a morphology (causing skews in angles, etc.) which is complex by default.

In formula 33 (one example of which is shown in Figure 28), changing the limit variable controls the degree of waviness of the outer layer. Changing the limit variable in Figure 1 changes the shape of one end and of the design in the circular center of the image. Figures 38 and 39 shows an interesting phenomenon associated with changing the intercellular constant ( $\nu$ ). The formulas for both of these figures are the same, but the real parts of  $\nu$  are slightly different. Observe that this change in  $\nu$  can account for the appearance (or lack of it) of one single structure, leaving the rest of the image unaffected. It is also interesting to note that amidst all the striking complexity of most figures there are areas which are structurally very simple.

## 3. Time series: development through function changes

To simulate the time course of development, where the co-regulation of gene products changes with time, the basic algorithm was iterated, resulting in a 'movie', where each frame was created using a slightly modified function  $\Delta\Phi$  (since in this model the DNA of the organism is represented by the function). This provides a continuous image of morphogenesis through time. The function can be changed continuously, or in discrete jumps, along one or more parameters.

A custom program was written in C, on a Sun-4, to generate frames using the same Julia set algorithm, and display them rapidly using the *Khoros* package (produced by the University of New Mexico). The results cannot adequately be represented in the static medium of paper (videotapes are available from the author), but descriptions of the time series (called 'movies' below) that were made can be instructive.

The movies were made with the parameters shown in Table II. Each movie consists of iterations of some formula, where all but one parameter is held constant. The remaining parameter is varied in small steps, and for each value of that parameter, a complete morphology is generated. These frames are then played back in order. In each movie, the choice of step size of the varying parameter is arbitrary. Smaller step sizes result in movies with better grain (smoother transitions), but requiring correspondingly longer generation times.

In general, most movies consist of periods of slow, smooth, continuous change interspersed with periods of very rapid major changes. These rapid changes generally occur at the beginning of the movie, though some movies exist where there is a rapid period of change in the middle (corresponding to the drastic morphological alterations of metamorphosis, in biological forms). Throughout, it is seen that certain structures (usually the outermost membrane) stay relatively constant in shape. Most movies show a shape that is generally static in size, while some have periods of growth. Some movies eventually settle down to a state where they change very little, corresponding to a complete morphology—the end of development. Note though

**Table II.** Movie specifications

No.	Formula	X limits	Y limits	$\nu$ value	i-limit
1	$z = z(z^6 + z^2) + bz^{8.5} + \nu$ a and b are real numbers. a goes from 0.0 to 1.0, while simultaneously b goes from 1.0 to 0.0 in equal steps, each such pair (a,b) defining a single frame of the movie.	-2.0 to 2.0	-2.0 to 2.0	(0.5,0)	100
2	$z = z^{5.5} + \cos(z) + \nu$ real ( $\nu$ ) stays at 0.0. Imaginary ( $\nu$ ) goes from 0.0 to -0.8. Each value of $\nu$ defines a single frame of the movie.	-1.4 to -0.9	-0.5 to 0.22	100	
3	$z = z^2 + \sin(z) + \nu$ imaginary ( $\nu$ ) stays at 5.5. Real ( $\nu$ ) goes from 3.0 to 3.5. Each value of $\nu$ defines a single frame of the movie.	-2.0 to 2.0	-2.0 to 2.0	100	
4	$z = az^{8.5} + b[\sin(z^{0.5}) + z^3] + \nu$ for each f from 0 to 160, $a = f \cdot 0.01$ , $b = 1 - f \cdot 0.01$ . Each (a,b) pair defines a single frame of the movie, when plugged into the formula.	-4.0 to 4.0	-4.0 to 4.0	(0,0)	100
5	$z = az^{1/z} + bz^{8.5} + \nu$ a and b are real numbers. a goes from 0.0 to 1.0, while simultaneously b goes from 1.0 to 0.0 in equal steps, each such pair (a,b) defining a single frame of the movie.	-5.0 to 5.0	-5.0 to 5.0	(0,0)	100
6	$z = a \cdot [z^{2.6} + \sin(z) + (\tilde{e})^{1.4} + \nu] + b \cdot [z^{2.5} + \sin(z) + (\tilde{e})^{0.7} + \nu]$ for each frame, a goes from 0.0 to 1.0, while simultaneously b goes from 1.0 to 0.0, $\nu$ goes from (-0.2,2.7) to (0.2,1.7) (real and imaginary components simultaneously), and the i-limit goes from 18 to 20.	-8.0 to 8.0	-8.0 to 8.0		
7	$z = z^{1.5} + a + \nu$ a goes from 0 to 30	-8.0 to 8.0	-8.0 to 8.0	(0,0)	100
8	$z = z^a + z \cdot z^{1/z} + \nu$ a goes from 0 to 3.0.	-8.0 to 8.0	-8.0 to 8.0	(0,0)	100
9	$z = z^3 + a \cdot z + \sin(a \cdot z)$ a goes from -10.0 to 10.0	-8.0 to 8.0	-8.0 to 8.0	(0,0)	100
10	$z = 4 \cdot z^3 + 3 \cdot z + \nu$ the imaginary part of $\nu$ stays at 0.0, while the real part of $\nu$ goes from 0.0 to 3.3.	-1.3 to 1.3	-1.5 to 1.5	100	
11	$z = z \cdot z + b \cdot z^3$ a goes from 3 to 4.8 while simultaneously b goes from 4 to 5.8.	-1.3 to 1.3	-1.5 to 1.5	(0,0)	100
12	$z = e^{1/z} + z^{3.5}$ limit goes from 5 to 90.	-2.0 to 2.4	-2.2 to 2.0	(0,0)	
13	$z = e^{1/a} z + a \cdot z$ a goes from 1.5 to 3.1.	-3.0 to 3.0	-3.0 to 3.0	(0,0)	100
14	$z = z^a + z^{-a}$ a goes from 3.0 to 7.0.	-3.5 to 3.5	-3.5 to 3.5	(0,0)	100

that even in this state, very minor modifications can be seen from time to time (biological maintenance). All these characteristics are very similar to the properties of real biological development. Through a large series of experiments, it was determined that the formula is the most interesting parameter to vary.

For example, movie 1 shows some interesting morphogenetic changes going on within the shape (reminiscent of the rearrangements accompanying gastrulation); another stunning feature appears ~75% of the way through the movie: a small part of the interior (on both sides of the axis of symmetry) acquires its own independent membrane, moves outward, breaks through

the outer membrane of the main figure (which then slowly rejoins to reform perfectly), moves away, and disintegrates. Movie 2 shows a close-up of a membrane disjunction—one can observe the kinetics of the outer and inner layers as they slowly split and spread apart from each other.

Movie 3 shows several interesting membrane properties (below, ‘membrane’ denotes tissue layers which separate macroscopic compartments, not cell membranes). The outermost membrane is seen to consist actually of five separate layers, which shrink inwards one at a time; the result of these membrane movements is a circular sack with four separate but identical regions, each possessing its own set of membranes.

Throughout the movie a region at the center of the embryo is seen to be in intimate contact with, and to change synchronously with, the deforming membranes. Movie 4 shows several interesting things. Very little change is seen until frame 65, at which point some drastic changes occur (reflecting the kinds of processes that can lead to metamorphosis). Two, and then four detachments (as in movie 1) occur. At the same time, the outer layer expands greatly in size. Movie 5 shows some continuous tissue growth, without the significant morphological rearrangements seen in movies 1 and 4. Movie 6 shows some interesting stalk preparations (a single stalk splitting into two shoots).

Movie 7 shows a circular outer layer studded with spikes. As the time progresses, new spikes are continually added. This always happens in the same spot, with the other spikes spreading out radially to make room for it. Movie 8 shows a mostly filled solid structure metamorphose into an intricately shaped sparse one. Movie 9 shows a worm-like shape with cyclic changes in the morphology of the outer layer. Movies 10 and 11 show different modes of ternary ‘mitosis’—a division of a roughly circular structure into three daughter structures, with partitioning of the internal components.

The fact that it is possible to make these movies is interesting since the functions themselves are highly non-linear—i.e. they are chaotic:  $|f(x) - f(x + \Delta x)|$  is large even for small  $\Delta x$ . Thus it was a surprise to the author to discover that a relatively large step size is enough to produce a smooth transition between frames, resulting in a continuous movie. It could have been the case that given the non-linear nature of these functions, small changes in the function produced images that were very different, thus making it impossible to produce a smoothly changing movie.

There are two basic ways to produce a movie. One is for each frame to represent a small change in some one parameter in function  $f()$ . The other is to produce a transition from one form to another. Suppose that one form is produced by function  $f()$ , and the other is produced by a function  $g()$ . One can then produce a smooth transition from form  $f()$  into form  $g()$  by introducing two real constants  $a$  and  $b$ , where in each frame  $a$  goes from 0.0 to 1.0, while simultaneously  $b$  goes from 1.0 to 0.0. Thus, in the beginning  $f()$  dominates, and at the end of the movie,  $g()$  dominates. The magnitude of the step size in changing  $a$  and  $b$  (the grain) determines the number of frames, and thus how continuous the transformation from one shape to the other is. For each frame, the function iterated becomes:

$$z = a \cdot f(z) + b \cdot g(z)$$

It is interesting to see that different step sizes are needed to produce continuous movies between different shapes. That is, there are shapes which easily evolve one into the other (e.g. Figures 11 and 12 are easily interconvertible), and there

are shapes which do not (e.g. the shape produced by  $z = \sin(z)$  is very difficult to convert into  $z = z^{9.5}$ ). Thus, these morphologies form ‘natural kinds’ (much as real organisms do), some of which are more closely related than others. This is all a higher-order property of the morphology, and cannot be determined directly by inspection from the formula itself. Thus, formulas expressing genetic interactions form obvious groups, on the basis of the morphologies they give rise to.

The grain size necessary to produce a continuous movie is thus a measure of the closeness between two morphologies, and is analogous to evolutionary distance in real organisms.  $z = z^{9.5}$  and  $z = \sin(z)$  are an example of two far-removed morphologies;  $z = z^6 + z^2$  and  $z = z^{8.5}$  are an example of two closely related ones. Interestingly, movie 6 (which is a conversion between Figures 11 and 12) shows that most of the change occurs very late in the sequence; in this scheme it is analogous to an evolutionary change in gene interactions, the effects of which are relatively minor and consist of a change late in development.

There may also be regions (e.g. some of the early regions in movie 1) that are discontinuous, and stay discontinuous no matter how fine a grain is used. This would represent forms that cannot arise from each other as a result of evolutionary processes.

#### 4. Randomness: dealing with perturbations

Errors in positional information in field theories have been studied (Lewis *et al.*, 1977). It is also possible to use this model to explore the implications of field-directed morphogenesis for the amazing stability and resistance to perturbations that real embryos exhibit. So far, the model has assumed that field values (positions) can be read exactly. This condition will be referred to as  $M_0$ . Some interesting results can be obtained when this is altered, in one of two ways.

The first method,  $M_1$ , corresponds to an inherently imprecise (fuzzy) positional information. This would correspond, for example, to a morphogen gradient that tends to spread out and become less sharp with time, or a cell’s field-reading mechanism that operates with some intrinsic error. In the implementation, this is done by using  $\{\text{type} = \phi(z + \Delta z)\}$  instead of  $\{\text{type} = \phi(z)\}$ : for each position, the function is applied not to the position itself, but to the position plus some small offset. If the offset is random, this produces a randomly distributed fuzziness in position (an inability of the cell to determine precisely where it is). If the offset is not random, it can be described by a function which corresponds to a positional information mutant (whose cells make a consistent error in reading positional field values).

The second method,  $M_2$ , is to model an inherently precise field, which is read by cells, some component of which distorts the positional information, and other components of which do not. The implementation then looks like  $\{\text{type} = \phi(z, z + \Delta z)\}$ : the type is a function of the real field value, but also of a slightly

distorted field value. The distortion can be interpreted as described in the previous paragraph.

Several of these types of experiments were done. Consider, for example, the form produced by  $z = z^3$ . (Figure 44 shows the morphology as computed from  $M_0$ ). A plausible initial hypothesis as to what would happen if one added a small, random offset to each point value is that the overall shape would be the same, but would be more fuzzy and diffuse, with less precise detail. Interestingly, this is not what happens. Figure 45 shows the figure as computed from  $M_1$ , with each  $\Delta z = z \pm$  a random number of range  $\log(z)$ . Note that part of the image is completely untouched, while another part is duplicated, and spatially shifted. One of the copies is more diffuse than the other, suggesting primary and supernumerary versions of the structure.

Figure 46 shows the morphology produced by formula 7 (at double scale) as computed from  $M_0$ . Note the sharp and well-defined edges, but lack of horizontal or vertical straight lines. Figure 47 shows the same thing computed from  $M_2$  (with each  $\Delta z =$  a random number between  $\pm z^{0.01}$ ). Note the fact that the interior detail has been obliterated by a clear rectangle; note also the 'picture-frame' rectangle of fuzzy pattern around it, and the perfect (unchanged) detail outside that. It is interesting that adding a random component to these functions is able to produce a straight edge, where there was none before.

The implication of this is that errors in reading the positional information field produce much more complicated effects than just fuzziness in the resulting image. They can result in multiple copies of certain parts of the morphology, as well as complicated spatial patterns of regions of imprecise and precise structures. Some regions of the field are very resistant to perturbations; some are not. In all cases there is a tolerance to such influences, since the results remain the same over a wide range of magnitudes for the influences. This is consistent with the considerable resistance of embryos to outside perturbations, and especially with the fact that errors in reading the positional information field have been considered as an explanation for the production of supernumerary limbs at regeneration sites (Trainor, 1982; Sessions *et al.*, 1989). Thus, the duplication of certain (but not all) structures as a result of small differences in positional information seen in Figure 45 is consistent with the results of Sessions and Ruth (1990) who showed that implanting small beads into developing amphibian embryos (thus altering the position of various cells relative to a positional information field) can induce supernumerary limbs. These types of experiments suggest many empirical tests for the model.

## Future directions

Work is in progress to extend this model to three-dimensional ( $R^3$ ) space. This would require suitable definitions of the operations (as, for example, there is no unique definition of multiplication for  $R^3$ ). Another interesting biological feature to study is the organizer: it is possible to make areas of the field

special in some way (e.g. by making the errors in field position inversely proportional to distance from the organizer).

This model can be directly applied to real organisms by defining operations to correspond to a system in which the interactions between morphogenetically important genes have been worked out. This awaits definitive quantitative studies on morphological gene interactions.

Part II of this paper will discuss another model (which utilizes iterated dynamical systems to model cell migration without differentiation), as well as the characteristics of a much-expanded model of field-directed morphogenesis. Much empirically testable information may be derived from this model if it were possible to obtain formulas coding for a particular real biological morphology. This is known as the syntactic inference problem. Part III will present work currently in progress, which seeks to develop a method for obtaining the formula for an arbitrary biological image; this method utilizes biologically inspired algorithms such as neural networks and genetic algorithms. Part IV will present a vector force field approach to morphogenesis.

## Acknowledgements

Some of the software (for the Sun platform) used in this work was written by Alva Couch. I would also like to thank Alva Couch, Susan G. Ernst, Ben Levin, Jorge Gonzalez and Dmitry Grenader for helpful discussions. Color slides and videotapes are available from the author. I would also like to thank Julia Levin for proofreading.

## References

- Apter,M.J. (1966) *Cybernetics and Development*, Pergamon Press, New York.
- Axelrod,R. and Hamilton,W.D. (1981) The evolution of cooperation. *Science*, **211**(4489), 1390–1396.
- Bakowska,J. and Jerka-Dziadkowicz,M. (1980) Ultrastructural aspect of size dependent regulation of surface pattern of complex ciliary organelle in a protozoan ciliate. *J. Embryol. Exp. Morphol.*, **59**, 355–375.
- Bard,J. (1990) *Morphogenesis: The Cellular and Molecular Processes of Developmental Anatomy*. Cambridge University Press, New York.
- Beardon,A.F. (1990) Symmetries of Julia sets. *Bull. London Math. Soc.*, **22**, 576–582.
- Beardon,A.F. (1991) *Iteration of Rational Functions*. Springer-Verlag, New York.
- Bode,M.P. and Bode,H.R. (1980) Formation of pattern in regenerating tissue pieces of hydra attenuata I Head–body proportion regulation. *Dev. Biol.*, **78**, 484–496.
- Brandts,W.A. and Trainor,L.E.H. (1990a) A non-linear field model of pattern formation: intercalation in morphalactic regulation. *J. Theor. Biol.*, **146**, 37–56.
- Brandts,W.A. and Trainor,L.E.H. (1990b) A non-linear field model of pattern formation: application to intracellular pattern reversal. *J. Theor. Biol.*, **146**, 57–86.
- Brière,C. and Goodwin,B.C. (1990) Effects of calcium input/output on the stability of a system for calcium-regulated viscoelastic strain fields. *J. Math. Biol.*, **28**, 585–593.
- Bryant,S.V. and Iten,L.E. (1976) Supernumerary limbs in amphibians. *Dev. Biol.*, **50**, 212–234.
- Burlando,B., Vietti,R.C., Parodi,R. and Scardi,M. (1991) Emerging fractal properties in Gorgonian growth forms. *Growth, Dev. Aging*, **55**, 161–168.
- Burr,H.S. (1941) Field properties of the developing frog eggs. *Proc. Natl. Acad. Sci. USA*, **27**, 276–281.
- Conrad,M. (1981) Algorithmic specification as a technique for computing with informal biological models. *BioSystems*, **13**, 303–320.
- Cooke,J. (1972a) Properties of the primary organization field of *Xenopus laevis* part I. *J. Embryol. Exp. Morphol.*, **28**, 13–26

- Cooke,J. (1972b) Properties of the primary organization field of *Xenopus laevis* part II. *J. Embryol. Exp. Morphol.*, **28**, 27–46.
- Cooke,J. (1972c) Properties of the primary organization field of *Xenopus laevis* part III. *J. Embryol. Exp. Morphol.*, **28**, 47–56.
- Cooke,J. (1973a) Properties of the primary organization field of *Xenopus laevis* part IV. *J. Embryol. Exp. Morphol.*, **30**, 49–62.
- Cooke,J. (1973b) Properties of the primary organization field of *Xenopus laevis* part V. *J. Embryol. Exp. Morphol.*, **30**, 283–300.
- Cooke,J. (1973c) Morphogenesis and regulation in spite of continued mitotic inhibition in *Xenopus* embryos. *Nature*, **242**, 55–57.
- Cooke,J. (1975) The emergence and regulation of spatial organization in early animal development. *Annu. Rev. Biophys. Bioengng*, **4**, 185–217.
- Cooke,J. (1979) Cell number in relation to primary pattern formation in the embryo of *Xenopus laevis*. *J. Embryol. Exp. Morphol.*, **51**, 165–182.
- Cooke,J. (1981) Scale of body pattern adjusts to available cell number in amphibian embryos. *Nature*, **290**, 775–778.
- Dissado,L.A. (1990) A fractal interpretation of the dielectric response of animal tissues. *Phys. Med. Biol.*, **35**, 1487–1503.
- Düchting,W. and Vogelsaenger,T. (1984) Analysis, forecasting, and control of three-dimensional tumor growth and treatment. *J. Med. Syst.*, **8**, 461–475.
- Düchting,W. and Vogelsaenger,T. (1985) Recent progress in modelling and simulation of three-dimensional tumor growth and treatment. *BioSystems*, **18**, 79–91.
- Evans,J. (1986) *Mind, Body, and Electromagnetism*. Element Books, London.
- Feder,J. and Aharony,A. (eds) (1990) *Fractals in Physics*. Media Magic, CA.
- Frankel,J. (1974) Positional information in unicellular organisms. *J. Theor. Biol.*, **47**, 439–481.
- French,V. (1988) Gradients and insect segmentation. *Development*, **103** (Suppl.), 3–16.
- French,V., Bryant,P.J. and Bryant,S.V. (1966) Pattern regulation in epimorphic fields. *Science*, **193**, 969–981.
- Gardiner,D.M. and Bryant,S.V. (1989) Organization of positional information in the axolotl limb. *J. Exp. Zool.*, **251**, 47–55.
- Garfinkel,D. (1984) Modeling of inherently complex biological systems. *Math. Biosci.*, **72**, 131–139.
- Goel,N.S. and Rogers,G. (1978) Computer simulation of engulfment and other movements of embryonic tissue. *J. Theor. Biol.*, **71**, 103–140.
- Goel,N.S. and Thompson,R.L. (1988) *Computer Simulations of Self-organization in Biological Systems*. Macmillan, New York.
- Goodwin,B.C. (1985) *Developing organisms as self-organizing fields*. In Antonelli,P.L. (ed.), *Mathematical Essays on Growth and the Emergence of Form*. University of Alberta Press.
- Goodwin,B.C. (1988) Problems and prospects in morphogenesis. *Experientia*, **44**, 633–637.
- Goodwin,B.C. and Cohen,M.H. (1969) A phase-shift model for the spatial and temporal organization of developing systems. *J. Theor. Biol.*, **25**, 49–107.
- Goodwin,B.C. and Trainor,L. (1980) A field description of the cleavage process in morphogenesis. *J. Theor. Biol.*, **85**, 757–770.
- Goodwin,B.C. and LaCroix,N. (1984) A further study of the holoblastic cleavage field. *J. Theor. Biol.*, **109**, 41–58.
- Goodwin,B.C., Biere,C. and O'Shea,P.S. (1987) Mechanisms underlying the formation of spatial structures in cells. In Poole,P.K. and Trinci,A.P. (eds). *Spatial Organization in Eukaryotic Microbes*. Society for General Microbiology, Washington, DC.
- Gow,N.A.R. (1987) Polarity and branching in fungi induced by electrical fields. In Poole,P.K. and Trinci,A.P. (eds), *Spatial Organization in Eukaryotic Microbes*. Society for General Microbiology, Washington, DC.
- Green,D.M. (1991) Chaos, fractals, and nonlinear dynamics in evolution and phylogeny. *Trends Ecol. Evol.*, **6**, 333–337.
- Green,J.B.A., New,H.V. and Smith,J.C. (1992) Responses of embryonic *Xenopus* cells to activin and FGF are separated by multiple dose thresholds and correspond to distinct axes of the mesoderm. *Cell*, **71**, 731–739.
- Gutowitz,H. (1991) *Cellular Automata*. Media Magic, CA.
- Guyon,E. and Stanley,H.E. (1991) *Fractal Forms*. Media Magic, CA.
- Harris,A.K. (1990) Testing cleavage mechanisms by comparing computer simulations to actual experimental results. *Ann. NY Acad. Sci.*, **582**, 60–77.
- Harrison,R.G. (1918) Experiments on the development of the forelimb of *Ambystoma*, a self-differentiating, equi-potential system. *J. Exp. Zool.*, **25**, 413–462.
- Hart,T.N. and Trainor,L.E.H. (1989) Geometrical aspects of surface morphogenesis. *J. Theor. Biol.*, **138**, 271–296.
- Hart,T.N., Trainor,L.E.H. and Goodwin,B.C. (1989) Diffusion effects in calcium-regulated strain fields. *J. Theor. Biol.*, **136**, 327–336.
- Herman,G.T. and Rozenberg,G. (1975) *Developmental Systems and Languages*. North-Holland, Amsterdam.
- Iannaccone,P.M. (1990) Fractal geometry in mosaic organs: a new interpretation of mosaic pattern. *FASEB J.*, **4**, 1508–1512.
- Ishibashi,A., Aihara,K. and Kotani,M. (1988) Chaos in brain and neurons and an analysis on the fractal dimensions. *Japan. J. Med. Electron. Biol. Engng*, **26**, 57–61.
- Jaffe,L.F. (1979) Control of development by ionic currents. In Cone,R.A. and Dowling,J.E. (eds), *Membrane Transduction Mechanisms*. Raven Press, New York.
- Kauffman,S.A. (1969) Metabolic stability and epigenesis in randomly constructed genetic nets. *J. Theor. Biol.*, **22**, 437–467.
- Kiani,M.F. and Hudez,A.G. (1991) Computer simulation of growth of anastomosing microvascular networks. *J. Theor. Biol.*, **150**, 547–560.
- Krebs,J.R., Kacelnik,A. and Taylor,P. (1978) Test of optimal sampling by foraging great tits. *Nature*, **275**, 27–31.
- Kropf,D.L. and Caldwell,L. (1983) Cell polarity: endogenous currents precede and predict branching in the water mold *Achylya*. *Science*, **220**, 1385–1387.
- Lakirev,A.V. and Belousov,L.V. (1986) Computer modelling of gastrulation and neurulation in amphibian embryos based on mechanical tension fields. *Otogenes*, **17**, 636–647.
- Landini,G. (1991) A fractal model for periodontal breakdown in periodontal disease. *J. Periodont. Res.*, **26**, 176–179.
- Langton,C. (1990) *Artificial Life I*, *Proceedings of the 1st Artificial Life Conference*, Santa Fe Complexity Sciences Series, NM.
- Langton,C. (1991) *Artificial Life II*, *Proceedings of the 2nd Artificial Life Conference*, Santa Fe Complexity Sciences Series, NM.
- Lewis,J. Slack,J.M.W. and Wolpert,L. (1977) Thresholds in Development. *J. Theor. Biol.*, **65**, 579–590.
- Liebovitch,L.S. and Toth,T.I. (1990) Using fractals to understand the opening and closing of ion channels. *Ann. Biomed. Engng*, **18**, 177–194.
- Lindenmeyer,A. and Prusinkiewica,P. (1989) Developmental models of multicellular organisms. In Langton, *Artificial Life I*, pp. 221–247.
- Lord,E.M. and Sanders,L.C. (1992) Roles of the extracellular matrix in plant development and pollination. *Dev. Biol.*, **153**, 16–28.
- Lund,E.J. (1947) *Bioelectric Fields and Growth*. University of Austin Press, TX.
- MacDonald,N. (1983) *Trees and Networks in Biological Models*. Wiley, New York.
- Mainster,M.A. (1990) The fractal properties of retinal vessels. *Eye*, **4**, 235–241.
- Mandelbrot,B. (1982) *The Fractal Geometry of Nature*. Media Magic, New York.
- Matioli,G.T. (1987) Cancer clonality and field theory. *Haematol. Blood Transfus.*, **31**, 286–289.
- Makin,P. (1986) A new model for biological pattern formation. *J. Theor. Biol.*, **118**, 101–113.
- Meinhardt,H. (1982) *Modes of Biological Pattern Formation*. Academic Press, New York.
- Meinhardt,H. (1984) Models for positional signalling: the threefold subdivision of segments and the pigmentation pattern of molluscs. *J. Embryol. Exp. Morphol.*, **83**, 289–311.
- Mittenthal,J.E. and Trevarrow,W.W. (1984) Intercalary regeneration in legs of crayfish: proximal segments. *Dev. Biol.*, **101**, 40–50.
- Mittenthal,J.E. and Nuelle,J.R. (1988) Discontinuities of pattern and rules for regeneration in limbs of crayfish. *Dev. Biol.*, **126**, 315–326.
- Murray,J.D. and Oster,G.F. (1984) Cell traction models for generating pattern and form in morphogenesis. *J. Math. Biol.*, **19**, 265–279.
- Nagorcka,B.N. (1989) Wavelike isomorphic prepatterns in development. *J. Theor. Biol.*, **137**, 127–162.
- Nelson,T.R., West,B.J. and Goldberger,A.L. (1990) The fractal lung: universal and species-related scaling patterns. *Experientia*, **46**, 251–254.
- Nucitelli,R. (1984) The involvement of transcellular ion currents and electric fields in pattern formation. In Malacinsky,G.M. and Bryant,S.V. (eds), *Pattern Formation*. Macmillan, New York.
- Nucitelli,R. (ed.) (1986) *Ionic Currents in Development*. Alan R.Liss, New York.
- O'Shea,P.S. (1988) Physical fields and cellular organisation: field-dependent mechanisms of morphogenesis. *Experientia*, **44**, 684–694.
- Othmer,H.G. and Pate,E. (1980) Scale-invariance in reaction–diffusion models of spatial pattern formation. *Proc. Natl. Acad. Sci. USA*, **77**, 4180–4184.
- Oxaal,U., Murat,M., Boger,F., Aharony,A., Feder,J. and Jossang,T. (1987)

- Viscous fingering on percolation clusters. *Nature*, **329**, 32–37
- Palmer,A.R. (1957) Ontogenetic development of two olenellid trilobites. *J. Paleontol.*, **31**, 105–128.
- Partridge,D. and Lopez,P.D. (1984) Computer programs as theories in biology. *J. Theor. Biol.*, **108**, 539–564.
- Papageorgiou and Venieratos (1983) A reaction diffusion theory of morphogenesis, **100**, 57–59.
- Petitgen,H.-O. and Saupe,D (eds) (1988) *The Science of Fractal Images* Springer-Verlag, New York
- Pickover,C. (1990) *Computers, Pattern, Chaos, and Beauty*. St Martin's Press, New York.
- Pietronero,L. and Tosatti,E. (eds) (1986) *Fractals in Physics* North-Holland, Amsterdam.
- Prusinkiewicz,P. and Lindenmayer,A. (1990) *The Algorithmic Beauty of Plants*. Springer-Verlag, New York.
- Raff,R.A. and Kaufman,T.C. (1983) *Embryos, Genes, and Evolution*. Macmillan, New York.
- Ransom,R. (1981) *Computers and Embryos*. Wiley, New York.
- Ransom,R. (1984) Computer modelling of cell division during development using a topological approach. *J. Embryol. Exp. Morphol.*, **83**, 233–259.
- Raup,D.M. and Michelson,A. (1965) Theoretical morphology of the coiled shell. *Science*, **147**, 1294–1295.
- Rogers,G. and Goel,N.S. (1978) Computer simulation of cellular movements cell sorting, cell migration through a mass of cells, and contact inhibition *J. Theor. Biol.*, **71**, 141–166.
- Rozenberg,G. and Salomaa,A (1986) *The Book of L*. Springer-Verlag, New York.
- Russel,M.A. (1985) Positional information in imaginal discs: a Cartesian coordinate model. In Antonelli,P L. (eds), *Mathematical Essays on Growth and the Emergence of Form*. University of Alberta Press.
- Sander,L.M. (1987) Fractal growth. *Scient. Am.*, **256**, 94–100.
- Savel'ev,S.V. (1988) The mechanism of encoding positional information by neuroepithelial cells from the brain of amphibian embryos. *Dokl. Akad. Nauk CCCP*, **301**, 1479–1483
- Sernetz,M., Gelléri,B. and Hofmann,J (1985) The organism as bioreactor. *J. Theor. Biol.*, **117**, 209–230.
- Sessions,S.K. and Ruth,S.B. (1990) Explanation for naturally occurring supernumerary limbs in amphibians. *J. Exp. Zool.*, **254**, 38–47.
- Sessions,S.K. , Gardiner,D.M. and Bryant,S.V. (1989) Compatible limb patterning mechanisms in urodeles and anurans. *Dev. Biol.*, **131**, 294–301.
- Slack,J.M.W. (1919) *From Egg to Embryo* Cambridge University Press, New York.
- Smith,T.G.Jr, Behar,T.N., Lange,G.D., Marks,W.B. and Sheriff,W.H..Jr (1991) A fractal analysis of cultured rat optic nerve glial growth and differentiation. *Neuroscience*, **41**, 159–166.
- Tabin,C.J. (1991) Retinoids, homeoboxes, and growth factors: toward molecular models for limb development. *Cell*, **66**, 199–217.
- Tevlin,P. and Trainor,L.E.H. (1985) A two-vector field model of limb regeneration and transplant phenomena. *J. Theor. Biol.*, **115**, 495–513.
- Thom,R. (1983) *Mathematical Models of Morphogenesis*. Wiley, New York.
- Thompson,D.W. (1961) *On Growth and Form*. Cambridge University Press, New York.
- Thomson,K.S. (1988) *Morphogenesis and Evolution*. Oxford University Press, New York.
- Totafumo,J., Lumsden,C.J. and Trainor,L.E.H. (1980) Structure and function in biological hierarchies *J. Theor. Biol.*, **85**, 171–198
- Trainor,L.E. (1982) A field approach to pattern formation in living systems *Phys. Can.*, **38**, 117–120.
- Vaidya,P.G., Vaidya,V.G. and Martin,D.G. (1991) An application of the non-linear bifurcation theory to tumor growth modeling *Int. J. Bio-Med. Comput.*, **27**, 27–46.
- West,B. (1991) *Fractal Physiology and Chaos In Medicine*. Media Magic, CA
- West,B. and Goldberger,? (1987) Physiology in fractal dimensions. *Am. Scient.*, **75**, 354–???
- Witten,T.A..Jr and Sander,L.M (1981) Diffusion limited aggregation, a kinetic critical phenomenon. *Phys. Rev. Lett.*, **47**, 1400–1403.
- Witten,T A..Jr and Cates,M.E. (1986) Tenuous structures from disorderly growth processes. *Science*, **232**, 1607–1612.
- Wolpert,L. (1969) Positional information and the spatial pattern of cellular differentiation. *J. Theor. Biol.*, **25**, 1–47
- Wolpert,L. (1971) Positional information and pattern formation. *Cur. Top. Dev. Biol.*, **6**, 183–224
- Wolpert,L. (1989) Positional information revisited. *Development*, Suppl., pp. 3–12.
- Yates,K. and Pate,E. (1989) A cascading development model for amphibian embryos. *Bull. Math. Biol.*, **51**, 549–578.
- Zackson,S.L. and Steinberg,M.S. (1988) A molecular marker for cell guidance information in the axolotl embryo. *Dev. Biol.*, **127**, 435–442.

Accepted November 16, 1993

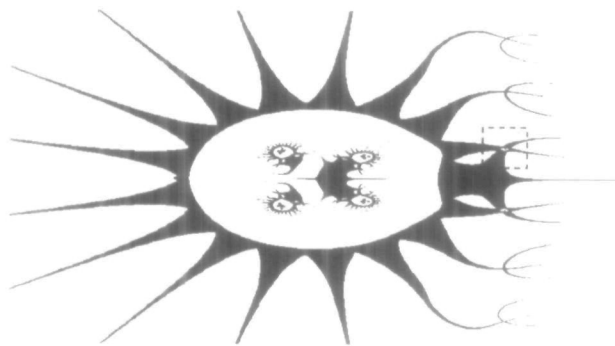


Fig. 1.

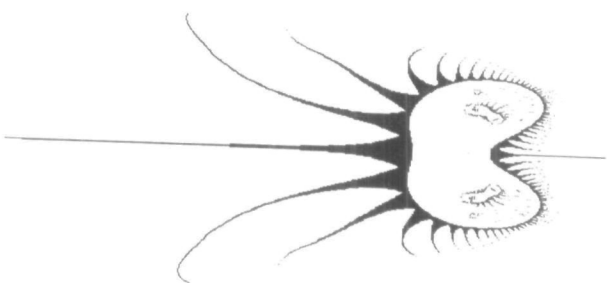


Fig. 5.

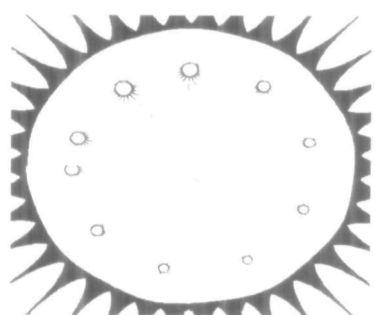


Fig. 2.

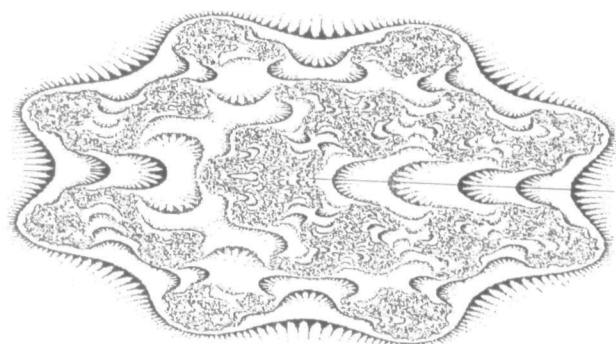


Fig. 6.

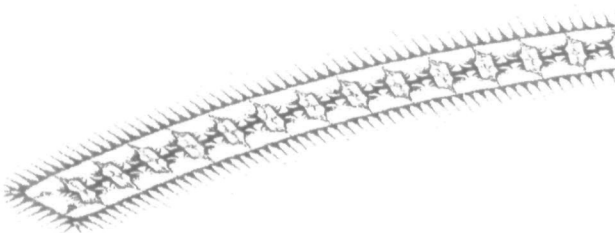


Fig. 3.

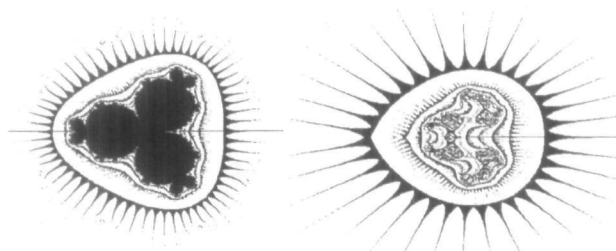


Fig. 7.



Fig. 8.

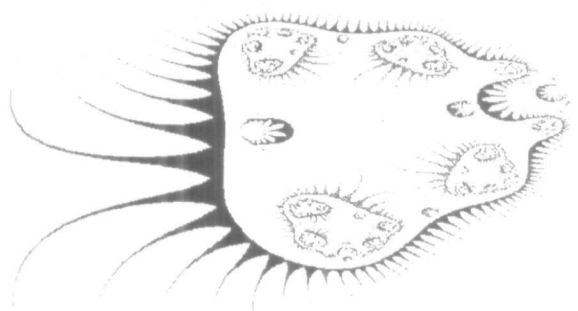


Fig. 4.

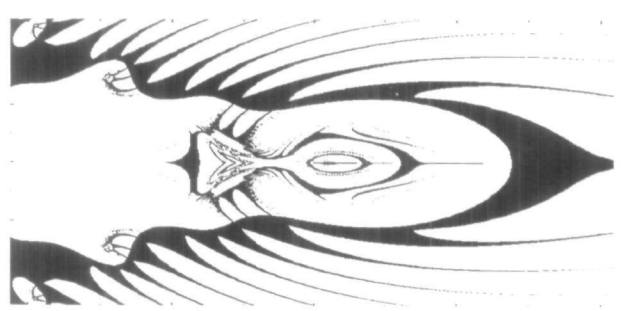


Fig. 9.

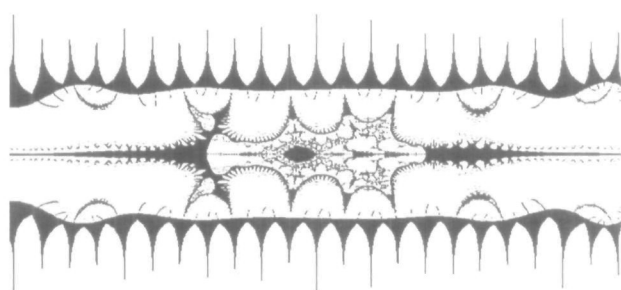


Fig. 10.

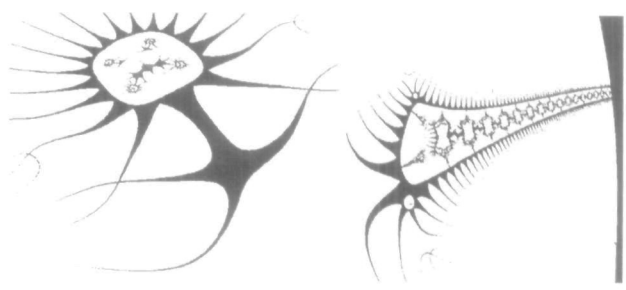


Fig. 16.

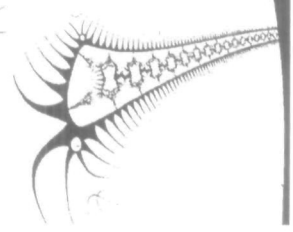


Fig. 17.

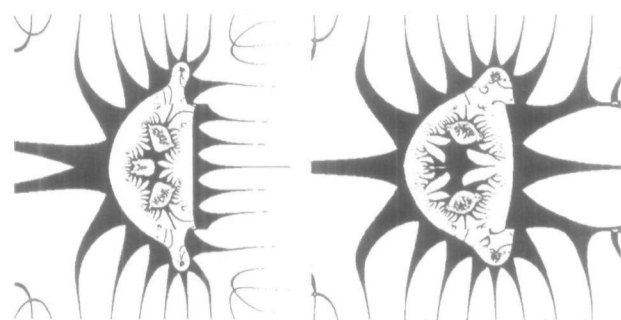


Fig. 11.

Fig. 12.

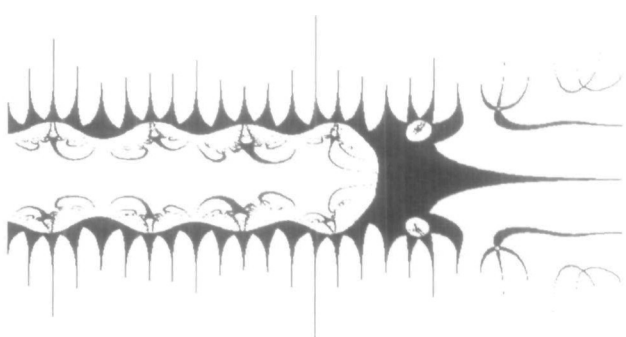


Fig. 18.

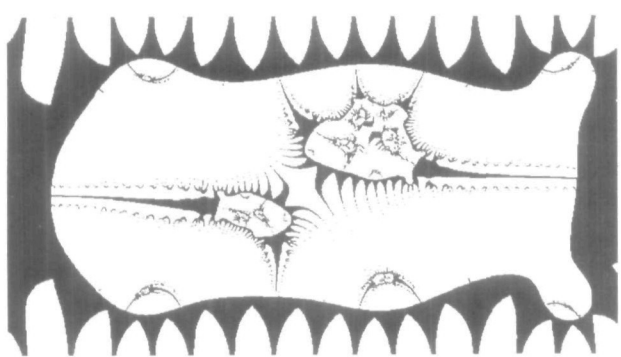


Fig. 13.

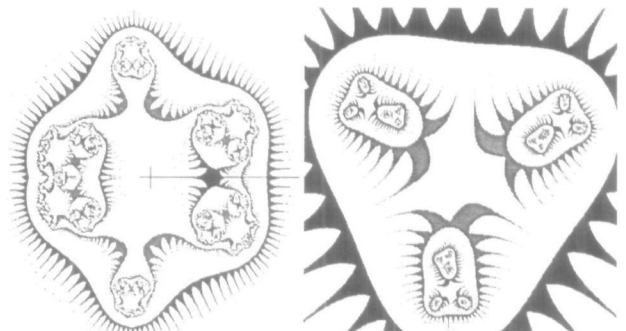


Fig. 19.



Fig. 20.

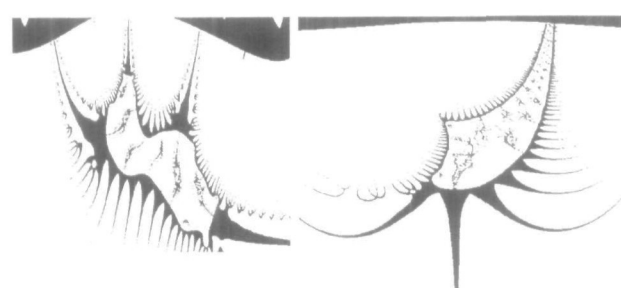


Fig. 14.

Fig. 15.

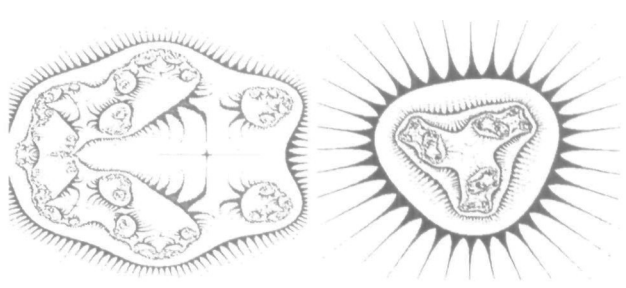


Fig. 21.



Fig. 22.

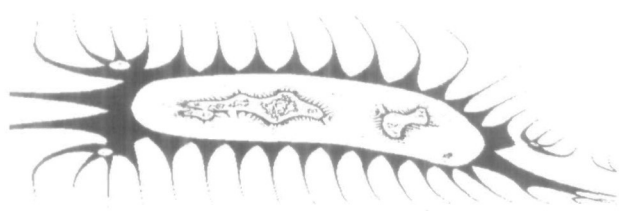


Fig. 23.

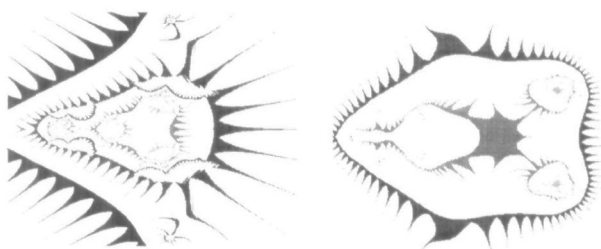


Fig. 29.

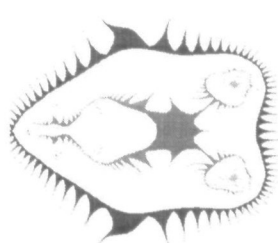


Fig. 30.

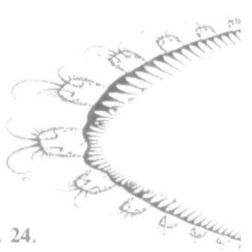


Fig. 24.

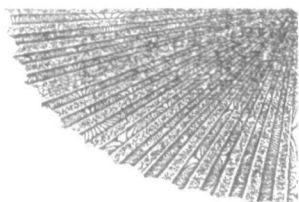


Fig. 25.

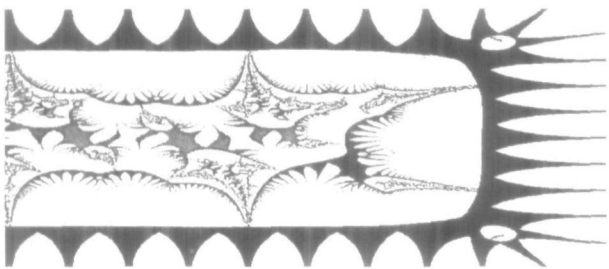


Fig. 26.



Fig. 31.

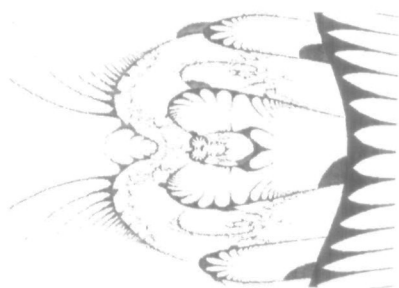


Fig. 27.

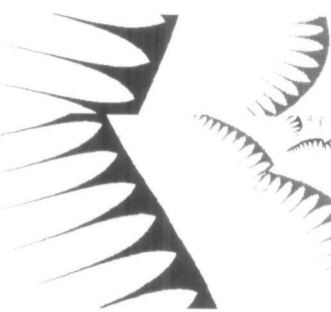


Fig. 32.

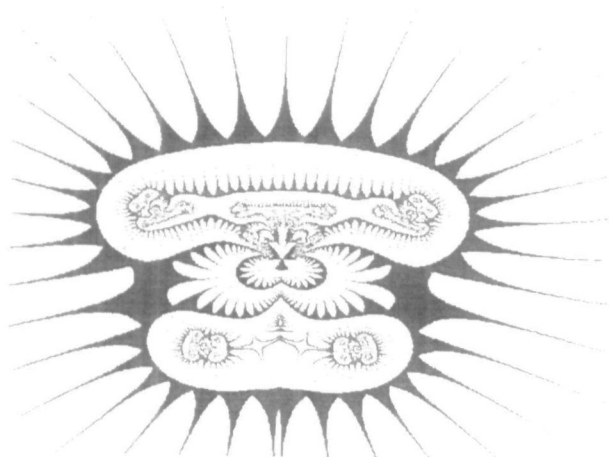


Fig. 28.

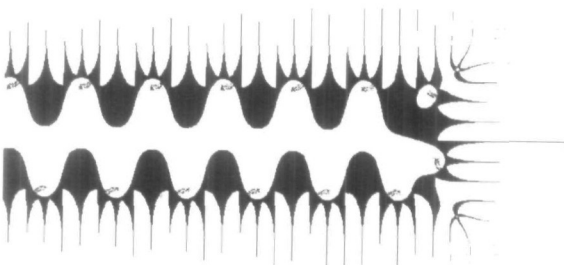


Fig. 33.

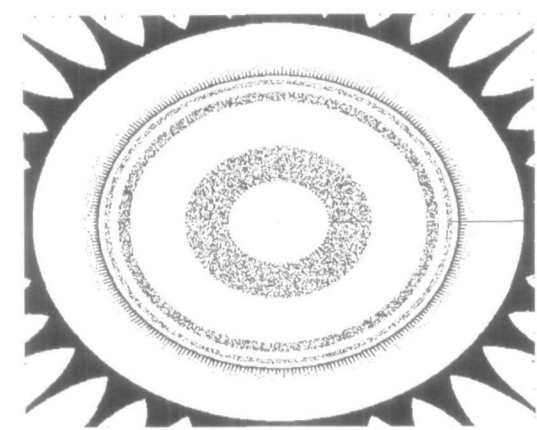


Fig. 34.

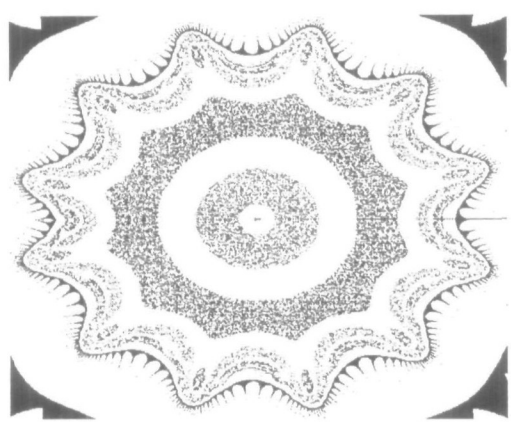


Fig. 35.

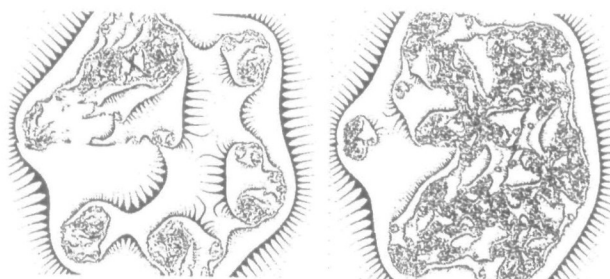


Fig. 36.

Fig. 37.

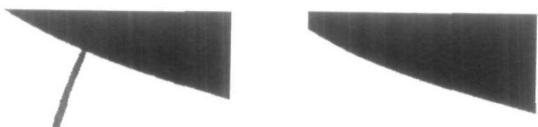


Fig. 38.

Fig. 39.

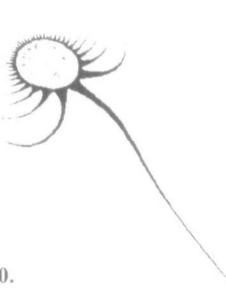


Fig. 40.

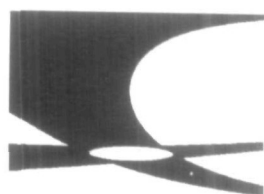


Fig. 41.

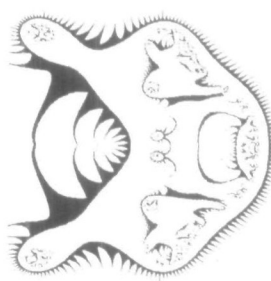


Fig. 42.

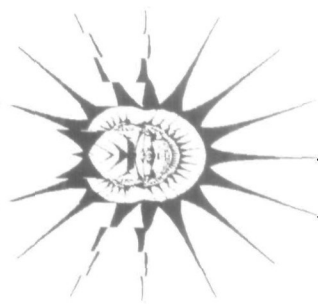


Fig. 43.

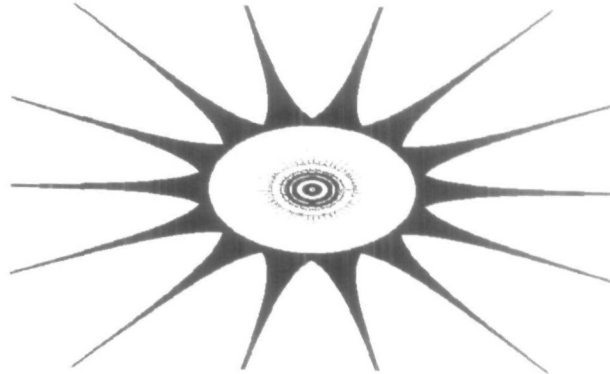


Fig. 44.

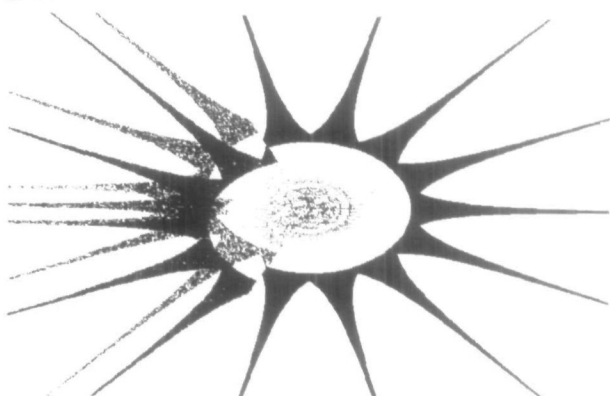


Fig. 45.

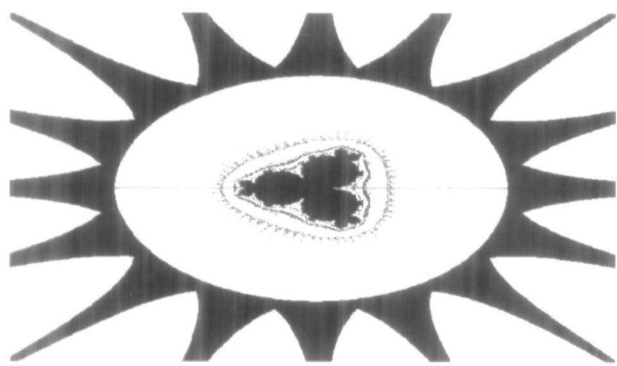


Fig. 46.

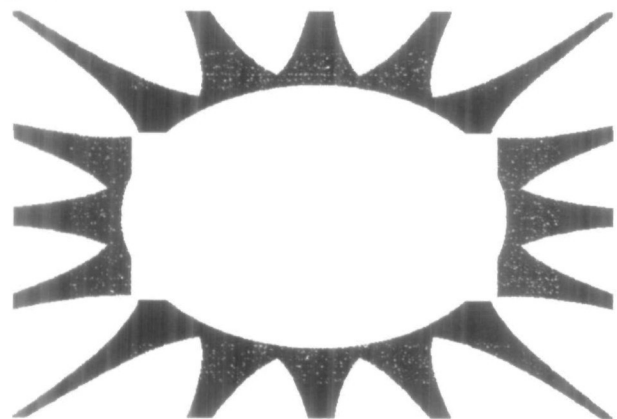


Fig. 47.

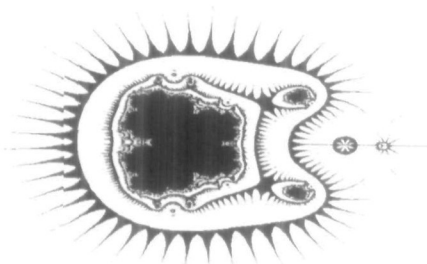


Fig. 48.

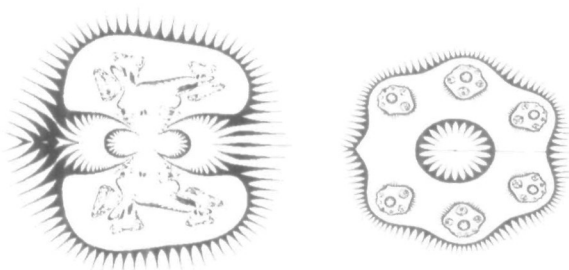


Fig. 49.

Fig. 50.

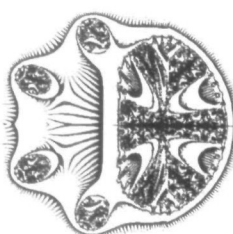


Fig. 51.

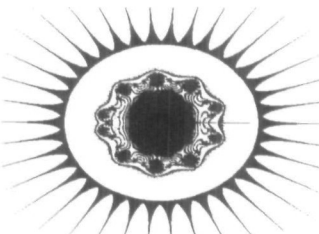


Fig. 52.

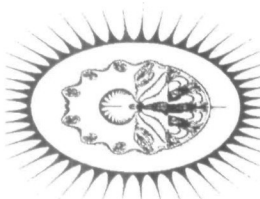


Fig. 53.

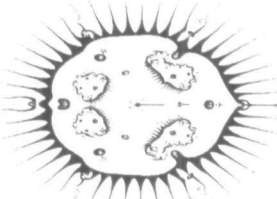


Fig. 54.



Fig. 55.

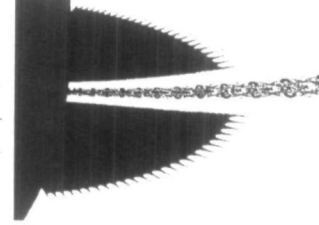


Fig. 56.

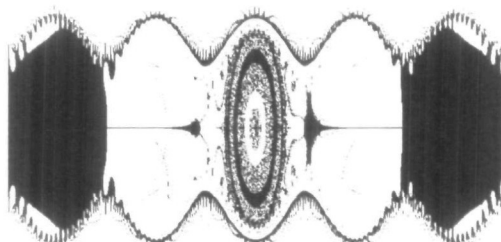


Fig. 57.

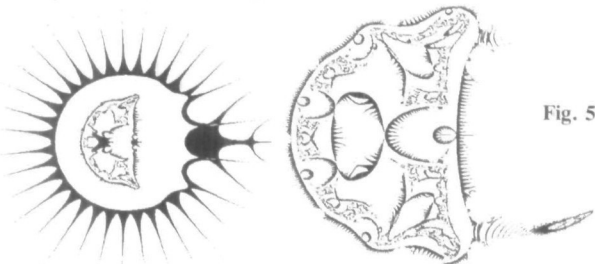


Fig. 58.

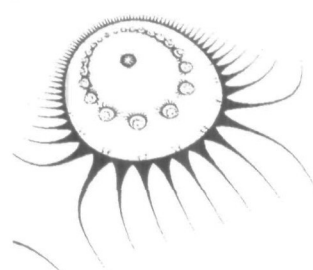


Fig. 59.

Fig. 60.



Fig. 61.

Dashed regions are examples of morphological aberrations.